Journal of Electronic Materials
SAND98-2591J

REDISTRIBUTION OF IMPLANTED DOPANTS IN GaN

X. A. Cao[1], R. G. Wilson[2], J. C. Zolper[3], S. J. Pearton[1], J. Han[4], R. J. Shul[4], D. J. Rieger[4], R. K. Singh[1], M. Fu[5], V. Scarvepalli[5], J. A. Sekhar[5], and J. M. Zavada[6]

[1]Department of Materials Science and Engineering, University of Florida, Gainesville, FL 32611 USA.
[2]Consultant, Stevenson Ranch, CA 91381 USA
[3]Office of Naval Research, Arlington, VA 22217 USA
[4]Sandia National Laboratories, Albuquerque, NM 87185 USA
[5]Micropyretics Heaters International, Inc. Cincinnati, OH 45212 USA
[6]European Research Office, USARDSG, London, England

ABSTRACT

Donor (S, Se and Te) and acceptor (Mg, Be and C) dopants have been implanted into GaN at doses of $3\text{-}5\times10^{14}$ cm^{-2} and annealed at temperatures up to 1450 °C. No redistribution of any of the elements is detectable by Secondary Ion Mass Spectrometry, except for Be, which displays an apparent damage-assisted diffusion at 900 °C. At higher temperatures there is no further movement of the Be, suggesting that the point defect flux that assists motion at lower temperatures has been annealed. Effective diffusivities are $\leq2\times10^{-13}$ $cm^2 \cdot sec^{-1}$ at 1450 °C for each of the dopants in GaN.

Introduction

Ion implantation is an effective technology for selected-area doping or isolation of GaN-based devices. As reviewed previously by Zolper,[1] implantation of donors at high dose ($>5\times10^{14}$ cm^{-2}) can be used to decrease source and drain access resistance in field effect transistors(FETs), at lower doses to create channel regions for FETs, while sequential implantation of both acceptors and donors may be used to fabricate p-n junctions. Two different device structures have been demonstrated using the latter method, namely a junction field-effect transistor[2] and a planar, homojunction light-emitting diode(LED).[3]

Due to the high vapor pressure of N_2 above GaN at the temperatures needed to activate implanted dopants,[4] it has proven necessary to either provide an overpressure of several kbars of N_2,[5] or to employ an AlN layer as an encapsulant during annealing.[6] The amount of residual lattice damage in the implanted GaN after annealing is a function of ion dose - for the relatively high doses needed for source/drain doping, it has been shown previously that annealing temperatures of ≥1400 °C are desirable.[7-12] We have found that Si, the most common n-type dopant, shows no detectable redistribution at 1400 °C, and that annealing at this temperature produces activation percentages of ≥90%.[13] Annealing at 1500 °C led to a reduction in both sheet electron concentration and electron mobility, which is consistent with self-compensation through site-switching of the Si. There is no available information on the other donor species, or on the possible acceptor dopants, in terms of their redistribution during ultra-high temperature annealing. In this paper we report on a Secondary Ion Mass Spectrometry (SIMS) study of GaN implanted with the group VI donors, S, Se and Te, and the acceptor species Mg, Be and

DISCLAIMER

DISCLAIMER

Portions of this document may be illegible in electronic image products. Images are produced from the best available original document.

C. Only Be is found to show redistribution during annealing, emphasizing the extremely good high temperature stability of dopants in GaN.

Experimental

Layers of GaN 2-3 μm thick were grown at ~1040 °C on c-plane Al_2O_3 by atmospheric pressure Metal Organic Chemical Vapor Deposition(MOCVD), using triethylgallium and ammonia. From x-ray diffraction and photoluminescence measurements we know this material is typical of the current state-of-the-art heteroepitaxial GaN.

The samples were implanted at 25 °C with 150 keV $^{24}Mg^+$, 80 keV $^{9}Be^+$, 80 keV $^{12}C^+$, 200 keV $^{32}S^+$, 300 keV $^{80}Se^+$, or 600 keV $^{128}Te^+$ ions, at doses of 3-5×10^{14} cm^{-2}. This puts the projected range, R_p, of the implanted species at least 1500 Å into the GaN in all cases, avoiding effects due to near-surface point defect injection. The samples were capped with ~1000 Å of reactively sputtered AlN, and annealed at temperatures of 1200-1450 °C under a N_2 ambient in the Zapper™ furnace described previously.[14] The dwell time at the peak temperature was ~10 sec. After annealing, the AlN was selectively etched in aqueous KOH at 80 °C.[15] The atomic distributions before and after annealing were measured by SIMS, and the data quantified using the as-implanted sample as a standard.

Results and Discussion

(a) Acceptor dopants

Figure 1 shows SIMS profile of implanted Mg in GaN, both before and after annealing at 1450 °C. Within the resolution of SIMS (~200 Å under these conditions)

there is no motion of the Mg. Using a simple $2\sqrt{Dt}$ estimation of the diffusivity at this temperature gives a value of $\leq 2\text{x}10^{-13}$ $cm^2 \cdot sec^{-1}$. This is in sharp contrast to its behavior in GaAs,[16-18] where the rapid diffusion of the Ga-site acceptors during annealing can only be suppressed by co-implanting a group V element to create a sufficient number of vacant sites for the initially interstitial acceptor ions to occupy upon annealing. This reduces the effective diffusivity of the acceptor and increases its electrical activation. The additional advantage gained from using a group V co-implant is that it maximizes occupation of the group III site by the acceptor.[19] In addition, implanted Mg in GaAs often displays outdiffusion toward the surface (in most case up, rather than down, the concentration gradient), leading to loss of dopant into the annealing cap.[20] This has been suggested to be due to non-equilibrium levels of Ga interstitials created by the implantation process. This mechanism is clearly absent for implanted Mg in GaN.

Figure 2 shows a series of profiles for ^{9}Be before and after annealing up to 1200 °C. Note that there is an initial broadening of the profile at 900 °C, corresponding to an effective diffusivity of ~$5\text{x}10^{-13}$ $cm^2 \cdot s^{-1}$ at this temperature. However there is no subsequent redistribution at temperatures up to 1200 °C. Implanted Be shows several types of anomalous diffusion in GaAs, including up-hill diffusion and movement in the tail of the profile, in addition to normal concentration-dependent diffusion,[18] which also result from the non-equilibrium concentrations of point defects created by the nuclear stopping process of the implanted ions. It appears that in GaN, the interstitial Be undergoes a type of transient-enhanced diffusion until these excess point defects are removed by annealing, at which stage the Be is basically immobile.

Carbon is typically a very slow diffuser in all III-V compounds, since it strongly prefers substitutional lattice sites.[18-21] In GaN it has been shown that it is possible to get

p-type conductivity in carbon-doped material, albeit with low hole concentrations.[22] In general however, GaN containing high concentrations of carbon is self-compensated, suggesting that carbon is occupying both Ga and N sites. Figure 3 shows that it is an extremely slow diffuser when implanted into GaN, with $D_{eff} \leq 2\times10^{-13}$ cm·sec^{-1} at 1400 °C.

(b) Donor dopants

Our previous results showed that Si is an effective donor impurity in implanted GaN.[13] Little work has been performed on the group VI donors, although Feng et al.[23] showed that Se displayed relatively high diffusion during growth by MOCVD at 1000 °C. Wilson reported some redistribution of implanted S after annealing at 700-1000 °C in relatively thin layers of GaN,[24] which might have been influenced by the high crystalline defect density in the material.

Figure 4 shows SIMS profiles before and after 1450 °C annealing of implanted S in GaN. There is clearly no motion of the sulfur under these conditions, which suggests that, as expected, the structural quality of the GaN may have a strong influence on the apparent diffusivity of dopants. The samples in the present experiment are much thicker than those employed in the previous work,[24] and the extended defect density will be correspondingly lower in the implanted region (~5×10^{8} cm^{-2} compared to ~10^{10} cm^{-2} in the thin samples).

The other group VI donors, Se and Te, have low diffusion coefficients in all compound semiconductors (for example $D_{Se}=5\times10^{-15}$ cm^2·sec^{-1} at 850 °C in GaAs),[18,19] and we find a similar result for these species implanted into GaN. Figure 5 shows the

SIMS profiles before and after 1450 °C annealing for Se, while Figure 6 shows similar data for Te. In both cases the effective diffusivity at this temperature is $\leq 2\times10^{-13}$ $cm^2 \cdot sec^{-1}$.

Summary and Conclusions

Most of the common acceptor and donor species have been implanted into GaN at room temperature, and subsequently annealed up to 1450 °C. With the exception of Be, which shows an apparent damage-assisted redistribution at 900 °C, none of the species show detectable motion under these conditions. This bodes well for the fabrication of GaN-based power devices such as thyristors and insulated gate bipolar transistors which will require creation of doped well or source/drain regions by implantation. The low diffusivities of implanted dopants in GaN means that junction placement should be quite precise and there will be less problems with lateral diffusion of the source/drain regions towards the gate. Finally, the results show the effectiveness of the AlN cap in protecting the GaN surface from dissociation, since if any of the surface was degraded during annealing, the implant profiles would no longer overlap.

ACKNOWLEDGEMENTS

The work of UF is partially supported by a DARPA/EPRI grant MDA 972-98-1-0006 (E. R. Brown/J. Melcher) and by an NSF grant DMR 9732865 (L. Hess). Sandia is a multiprogram laboratory operated by Sandia Corporation, a Lockheed-Martin company, for the US Department of Energy under contract No. DEAC04-94 AL 85000. The work of R. G. Wilson is partially supported by an ARO grant.

References

1. J. C. Zolper, in GaN and Related Materials, Vol. 2 of Optoelectronic Properties of Semiconductors and Superlattices. (Gordon and Breach, NY 1997); J. C. Zolper, S. J. Pearton, C. R. Abernathy, C. B. Vartuli, C. Yuan and R. A. Stall, Proc. Vol. 95-21 (Electrochemical Society, Pennington, NJ, 1995), pp 144-151; J. C. Zolper and R. J. Shul, MRS Bulletin 22 36 (1997); J. C. Zolper, Proc. Vol. 97-34 (Electrochemical Society, Pennington, NJ, 1997), pp 76-82; J. C. Zolper, R. J. Shul, A. G. Baca, S. J. Pearton, C. R. Abernathy, R. G. Wilson, R. A. Stall and M. Shur, Proc. Vol. 96-11 (Electrochemical Society, Pennington, NJ, 1996), pp 149-158; J. C. Zolper, J. Cryst. Growth 178 175 (1997).
2. J. C. Zolper, R. J. Shul, A. G. Baca, R. G. Wilson, S. J. Pearton and R. A. Stall, Appl. Phys. Lett. 68 2273 (1996).
3. H. P. Maruska, M. Lioubtchenko, T. G. Tetreault, M. Osinski, S. J. Pearton, M. Schurman, R. Vaudo, S. Sakai, Q. Chen and R. J. Shul, Mat. Res. Soc. Symp. Proc. 483 345 (1998).
4. See for example, N. Newman, Proc. Vol. 96-11 (Electrochemical Society, Pennington, NJ, 1996), pp 1-19; S. Porowski and I. Grzegory, in GaN and Related Materials, Vol. 2 of Optoelectronic Properties of Semiconductors and Superlattices (Gordon and Breach, NY 1997); T. Matsuoka, T. Sasaki and A. Katsui, Optoelectronics 5 53 (1990).
5. J. C. Zolper, J. Han, S. B. Van Deusen, R. M. Biefeld, M. H. Crawford, J. Han, T. Suski, J. M. Baranowski and S. J. Pearton, Mat. Res. Soc. Symp. Proc. 482 609 (1998).

6. J. C. Zolper, D. J. Reiger, A. G. Baca, S. J. Pearton, J. W. Lee and R. A. Stall, Appl. Phys. Lett. 69 538 (1996).

7. J. C. Zolper, J. Han, R. M. Biefeld, S. B. Van Deusen, W. R. Wampler, D. J. Reiger, S. J. Pearton, J. S. Williams, H. H. Tan and R. Stall, J. Electron. Mater. 27 179 (1998).

8. H. H. Tan, J. S. Williams, J. Zou, D. J. H. Cockayne, S. J. Pearton and R. A. Stall, Appl. Phys. Lett. 69 2364 (1996).

9. J. C. Zolper, M. H. Crawford, H. H. Tan, J. S. Williams, J. Zou, D. J. H. Cockayne, S. J. Pearton and R. F. Karlicek, Appl. Phys. Lett. 70 2729 (1997).

10. C. Liu, B. Mecnsching, M. Zeitter, K. Volz and B. Rauschenbach, Phys. Rev. B 57 217 (1997).

11. S. Strite, A. Pelzman, T. Suski, M. Leszczynski, J. Jun, A. Rockett, M. Kemp and K. J. Ebeling, Int. J. Nitride Semicond. Res. 2 17 (1997).

12. T. Suski, J. Jun, M. Leszczynski, H. Teisseyre, I. Grzegory, S. Porowski, J. M. Baranowski, A. Rockett, S. Strite, A. Stonert, A. Turos, H. H. Tan, J. S. Williams and C. Jagadish, Mat. Res. Soc. Symp. 482 817 (1998).

13. X. A. Cao, C. R. Abernathy, R. K. Singh, S. J. Pearton, M. Fu, V. Sarvepalli, J. A. Sekhar, J. C. Zolper, D. J. Rieger, J. Han, T. J. Drummond, R. J. Shul and R. G. Wilson, Appl. Phys. Lett. 73 (1998).

14. M. Fu, V. Sarvepalli, R. K. Singh, C. R. Abernathy, X. Cao, S. J. Pearton and J. A. Sekhar, Mat. Res. Soc. Symp. Proc. 483 345 (1998).

15. J. R. Mileham, S. J. Pearton, C. R. Abernathy, J. D. MacKenzie, R. J. Shul and S. P. Kilcoyne, Appl. Phys. Lett. 67 1119 (1995).

16. M. D. Deal and H. G. Robinson, Appl. Phys. Lett. 55 1990 (1989).

17. H. G. Robinson, M. D. Deal and D. A. Stevenson, Appl. Phys. Lett. 58 2000 (1991).

18. M. D. Deal, C. J. Hu, C. C. Lee and H. G. Robinson, Mat. Res. Soc. Symp. 300 365 (1993).

19. S. J. Pearton, Int. J. Mod. Phys. 7 4687 (1993).

20. H. G. Robinson, M. D. Deal, P. B. Griffin, G. Amaratunga, P. B. Griffin, D. A. Stevenson and J. D. Plummer, J. Appl. Phys. 71 2615 (1992).

21. S. J. Pearton and C. R. Abernathy, Appl. Phys. Lett. 55 678 (1989).

22. C. R. Abernathy, J. D. MacKenzie, S. J. Pearton and W. S. Hobson, Appl. Phys. Lett. 66 1969 (1995).

23. M. S. Feng, J. D. Guo and G. C. Chi, Proc. Vol. 95-21 (Electrochemical Society, Pennington, NJ, 1995), pp 43-49.

24. R. G. Wilson, S. J. Pearton, C. R. Abernathy and J. M. Zavada. Appl. Phys. Lett. 66 2238 (1995); R. G. Wilson, Proc. Vol. 95-21 (Electrochemical Society, Pennington, NJ, 1995), pp 152-162.

Figure Captions

Figure 1. SIMS profiles before and after annealing at 1450 °C of implanted Mg (150 keV, 5×10^{14} cm^{-2}) in GaN.

Figure 2. SIMS profiles before and after annealing at different temperatures of implanted Be (80 keV, 5×10^{14} cm^{-2}) in GaN.

Figure 3. SIMS profiles before and after annealing at 1400 °C of implanted C (80 keV, 5×10^{14} cm^{-2}) in GaN.

Figure 4. SIMS profiles before and after annealing at 1450 °C of implanted S (200 keV, 5×10^{14} cm^{-2}) in GaN.

Figure 5. SIMS profiles before and after annealing at 1450 °C of implanted Se (300 keV, 5×10^{14} cm^{-2}) in GaN.

Figure 6. SIMS profiles before and after annealing at 1450 °C of implanted Te (600 keV, 3×10^{14} cm^{-2}) in GaN.

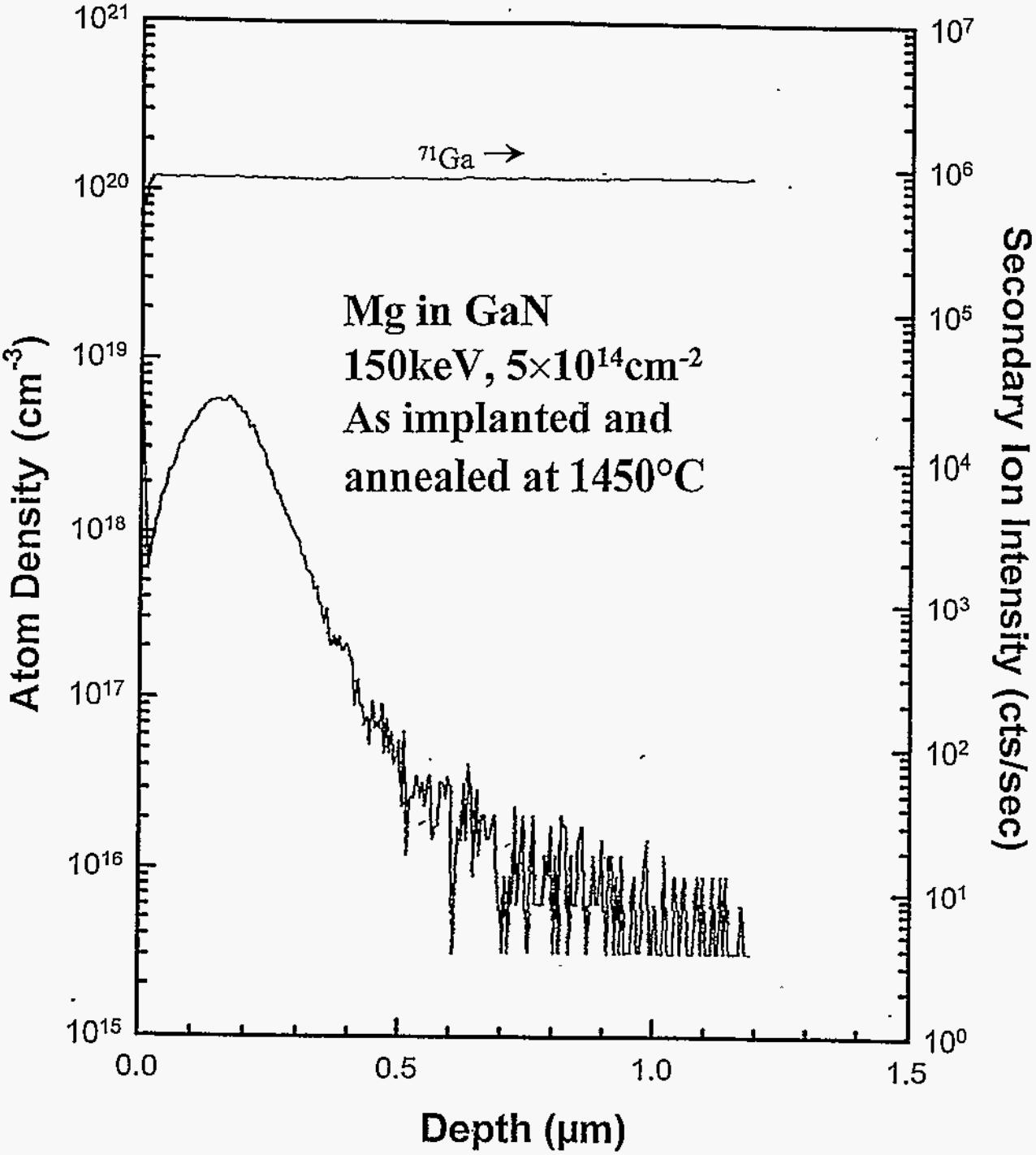
Mg in GaN
150keV, 5×10^14cm^-2
As implanted and
annealed at 1450°C
71Ga →
Atom Density (cm^-3)
Secondary Ion Intensity (cts/sec)
Depth (μm)
10^21
10^20
10^19
10^18
10^17
10^16
10^15
10^7
10^6
10^5
10^4
10^3
10^2
10^1
10^0
0.0
0.5
1.0
1.5

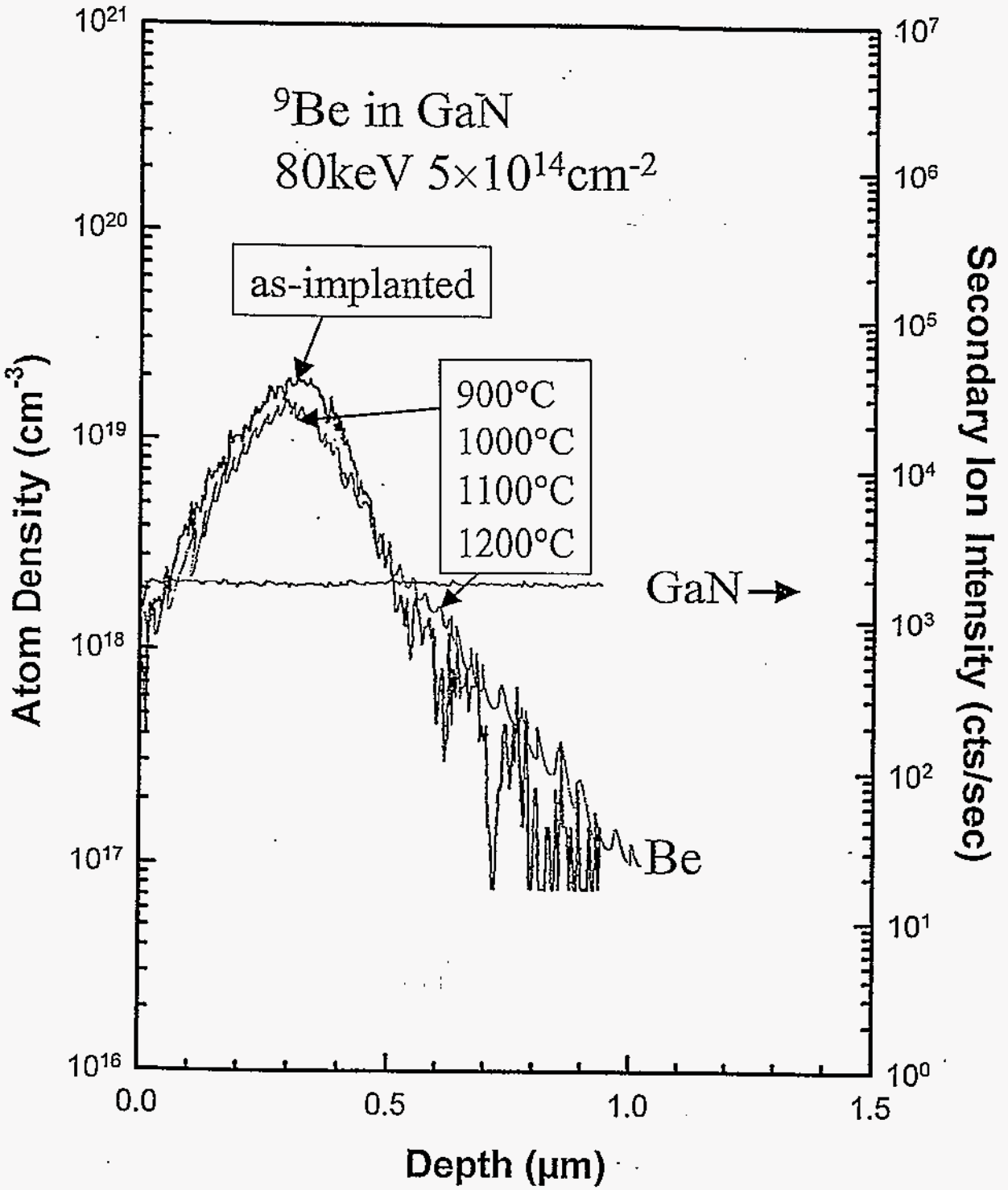
^{9}Be in GaN
80keV 5×10^{14}cm^{-2}
as-implanted
900°C
1000°C
1100°C
1200°C
GaN
Be
Atom Density (cm^{-3})
Secondary Ion Intensity (cts/sec)
Depth (μm)
10^{21}
10^{20}
10^{19}
10^{18}
10^{17}
10^{16}
10^7
10^6
10^5
10^4
10^3
10^2
10^1
10^0
0.0
0.5
1.0
1.5

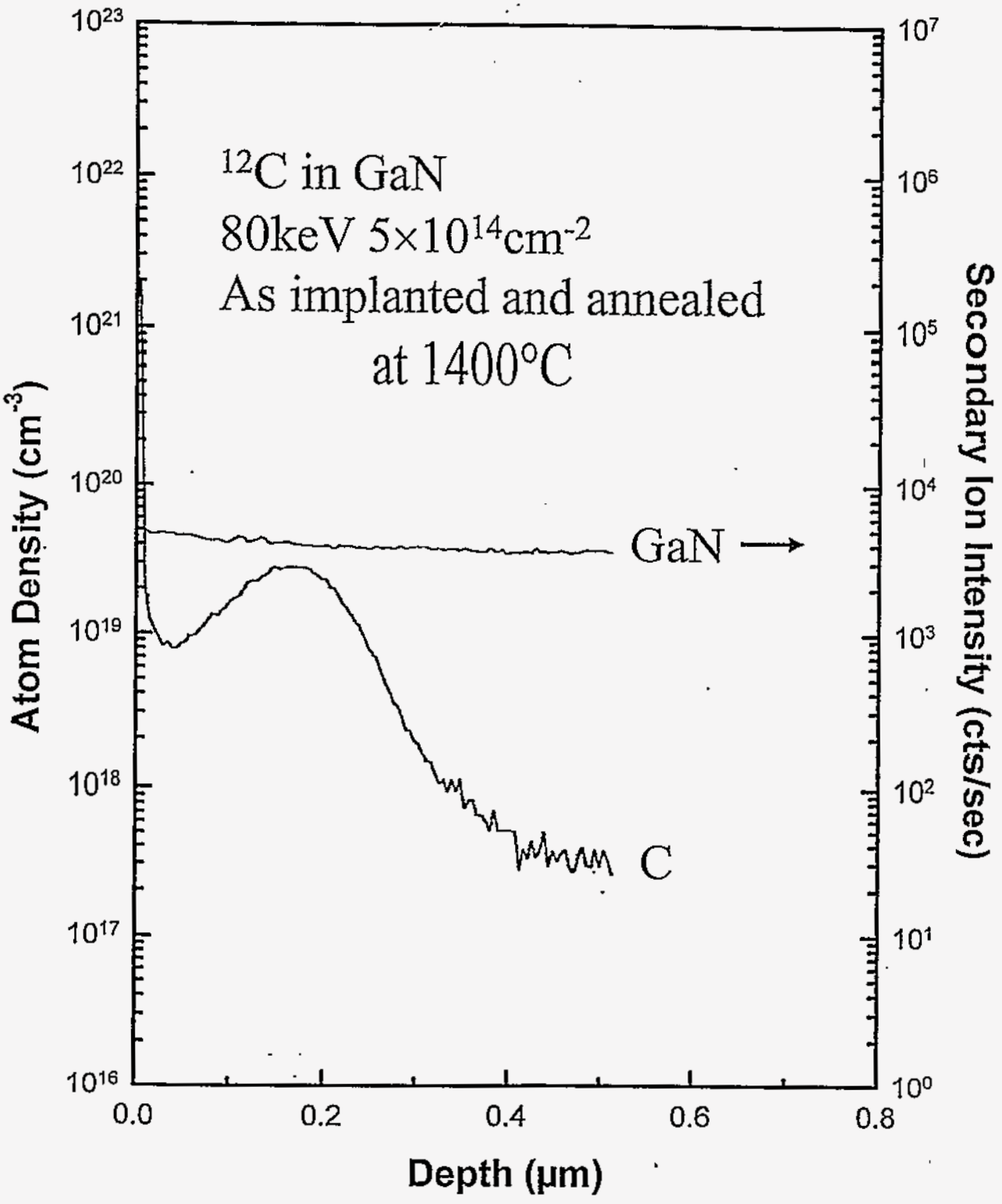
^{12}C in GaN
80keV 5×10^{14}cm^{-2}
As implanted and annealed
at 1400°C
GaN
C
Atom Density (cm^{-3})
Secondary Ion Intensity (cts/sec)
Depth (μm)
10^{23}
10^{22}
10^{21}
10^{20}
10^{19}
10^{18}
10^{17}
10^{16}
10^{7}
10^{6}
10^{5}
10^{4}
10^{3}
10^{2}
10^{1}
10^{0}
0.0
0.2
0.4
0.6
0.8

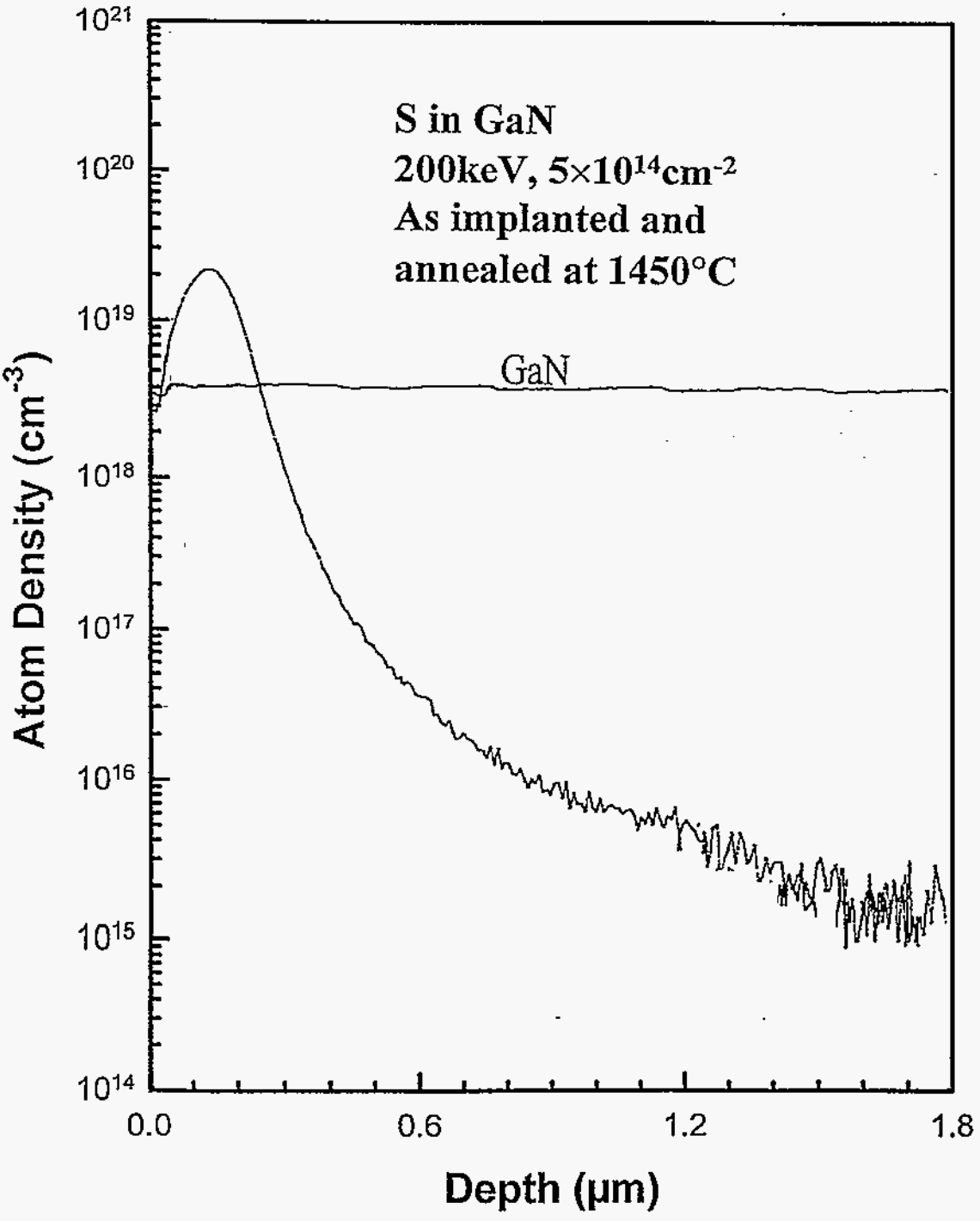
S in GaN
200keV, 5×10¹⁴cm⁻²
As implanted and
annealed at 1450°C
GaN
Atom Density (cm⁻³)
10²¹
10²⁰
10¹⁹
10¹⁸
10¹⁷
10¹⁶
10¹⁵
10¹⁴
0.0
0.6
1.2
1.8
Depth (μm)

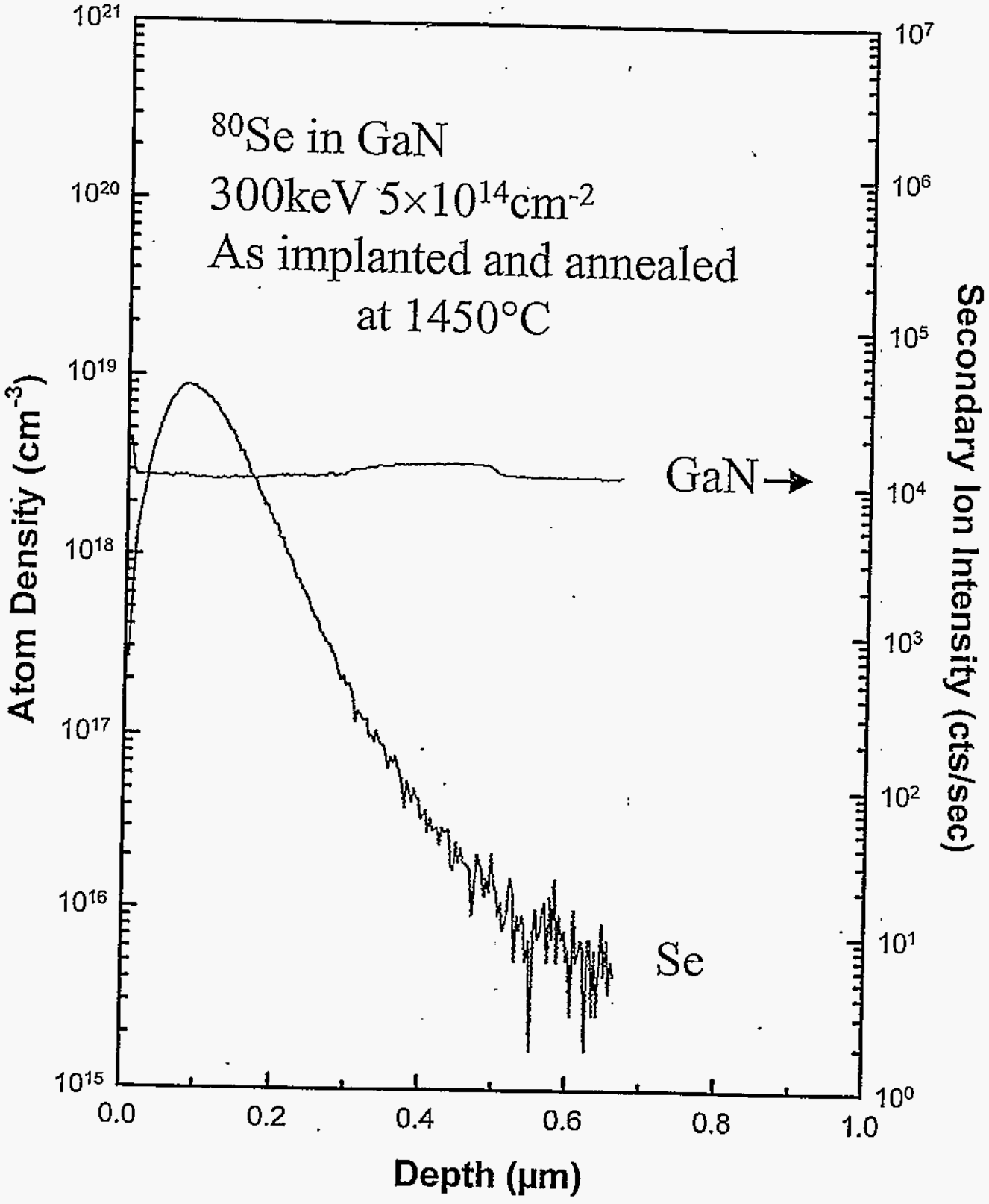
^{80}Se in GaN
300keV 5×10^{14}cm^{-2}
As implanted and annealed
at 1450°C
GaN
Se
Atom Density (cm^{-3})
Secondary Ion Intensity (cts/sec)
Depth (μm)
10^{21}
10^{20}
10^{19}
10^{18}
10^{17}
10^{16}
10^{15}
10^{7}
10^{6}
10^{5}
10^{4}
10^{3}
10^{2}
10^{1}
10^{0}
0.0
0.2
0.4
0.6
0.8
1.0

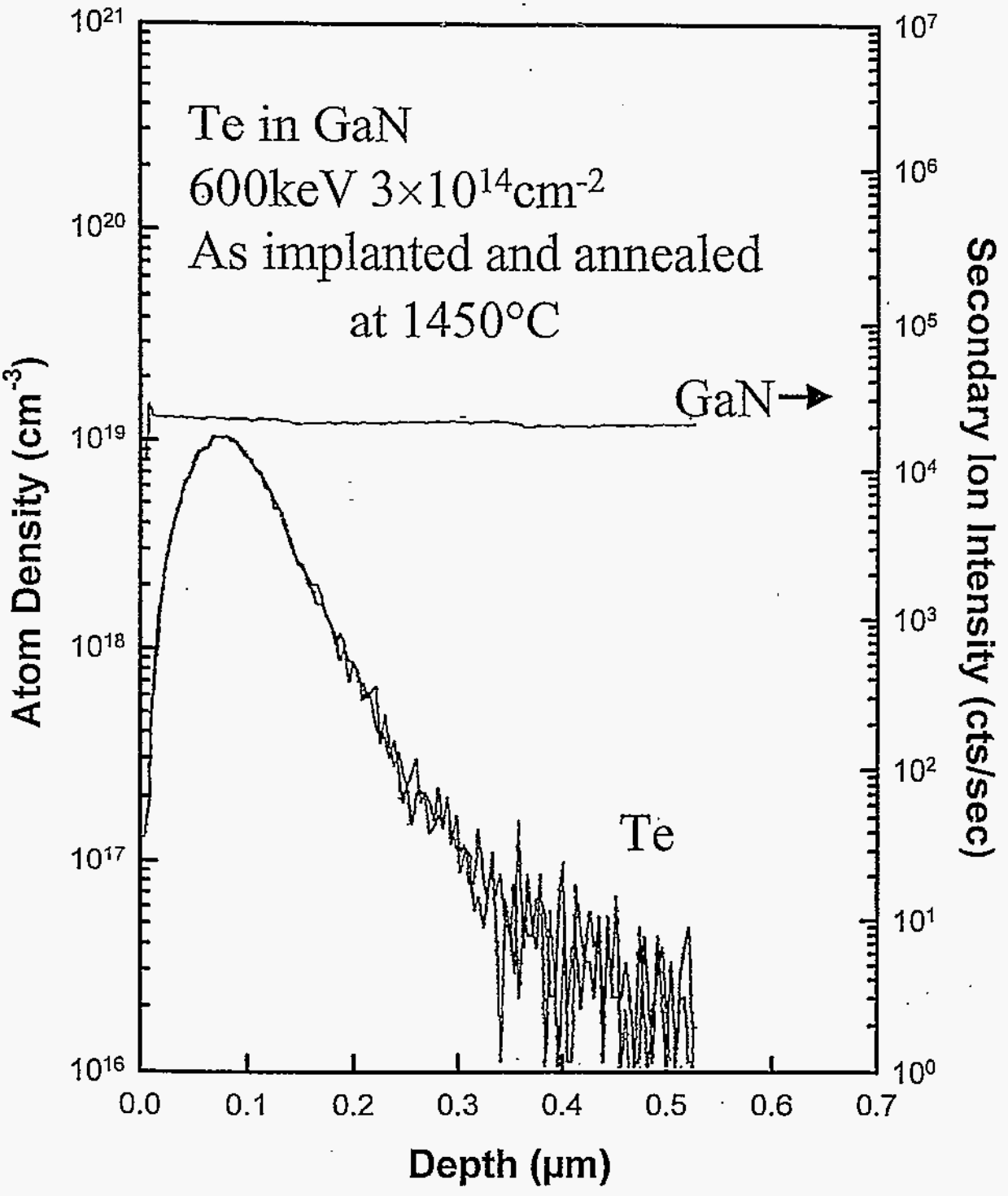
Te in GaN
600keV 3×10^14cm^-2
As implanted and annealed
at 1450°C
GaN→
Te
Atom Density (cm^-3)
Secondary Ion Intensity (cts/sec)
Depth (μm)
10^21
10^20
10^19
10^18
10^17
10^16
10^7
10^6
10^5
10^4
10^3
10^2
10^1
10^0
0.0
0.1
0.2
0.3
0.4
0.5
0.6
0.7